

Commentationes

An ICSCF Investigation of Walsh's Rules

Larilyn Zeller Stenkamp and Ernest R. Davidson

Chemistry Department BG-10, University of Washington, Seattle, Washington 98195 USA

Received March 27, 1973

The ICSCF method is applied to the calculation of orbital energies as a function of bond angle for several AH_2 molecules. The resulting orbital energy diagrams are quite similar in appearance to the canonical SCF results even though the sum of the ICSCF energies is the SCF energy. The method is also applied to Li_2O , CO_2 , HCN and a few AH_3 molecules with similar results. The sum of the ICSCF valence orbital energies generally correlates better with the equilibrium bond angle than does the similar sum of canonical orbital energies.

Key words: Walsh's rules – Orbital energies

Introduction

Rules for predicting the geometry and spectra of triatomic molecules have been formulated by Walsh [1] and Mulliken [2] in the molecular orbital language. Implicit in Walsh's formulation is a set of "binding energies", associated with the orbitals, having the property that changes in total energy are given approximately by changes in the sum of the orbital energies. Thus, in discussing geometry, Walsh assumed that the minimum total energy occurred where the sum of the orbital energies was minimum. Also, in discussing spectra, differences of orbital energies were used to predict the relative positions of excited states.

Within this context Walsh estimated in detail how the energy of each molecular orbital would vary with angle in various triatomic molecules. These estimates have proven to be fairly accurate although certain ones of them were significantly in error. Based on his detailed estimates, Walsh was able to correctly predict the geometry of most triatomic molecules.

Since these original papers, there have appeared innumerable articles attempting to formulate in a rigorous manner these superficially simple results. No attempt will be made to review these articles here since a review paper has recently been written by Buenker and Peyerimhoff [3]. Clearly the orbital energies as used by Walsh have many of the properties associated with orbital energies in the Hückel empirical interpolation schemes. Extended Hückel theory results do generally parallel the predictions of Walsh's rules (even when they are wrong) [4].

Within the Hartree-Fock framework the situation is more difficult. Let

$$h = -\frac{1}{2} \nabla^2 - \sum_A Z_A r_A^{-1} \quad (1)$$

$$F = h + 2J - K \quad (2)$$

be the one-electron and Fock operators respectively, and let

$$F\psi_i = \varepsilon_i \psi_i \quad (3)$$

and

$$h_{ii} = \langle \psi_i | h | \psi_i \rangle \quad (4)$$

define the canonical Hartree-Fock orbitals ψ_i with orbital energy ε_i and one-electron energy h_{ii} . Then the energy of a closed-shell molecule is given by

$$E = \sum_{i=1}^{N/2} (\varepsilon_i + h_{ii}) + V_N \quad (5)$$

where

$$V_N = \sum_{A < B} Z_A Z_B R_{AB}^{-1}. \quad (6)$$

Alternatively,

$$E = \sum_i 2\varepsilon_i + V_N - V_e \quad (7)$$

where

$$V_e = \sum_{i=1}^{N/2} (\varepsilon_i - h_{ii}) \quad (8)$$

is the electron-electron repulsion energy. Coulson and Neilson [5] proposed that the quantity $1/2(\varepsilon_i + h_{ii})$ be associated with the orbital binding energy of Walsh. While this works to some extent for AH_2 molecules where V_N does not change much with angle, it leads to quite erroneous results for AB_2 molecules such as OF_2 [6].

For many molecules the SCF orbital energy, ε_i , seems to work fairly well. Since the charge distribution tends to follow the nuclei, $V_N - V_e$ changes slowly with angle for non-ionic molecules. Peyerimhoff, Buenker and Allen [7] have shown that the sum of the valence orbital ε_i parallels the true energy dependence on angle for some AH_2 and non-ionic AB_2 molecules. Two well-known exceptions are Li_2O in which Walsh's formulation and the sum of the SCF orbital energies both fail to predict the linear geometry [6] and HCN for which the Walsh formulation makes a correct prediction, but the sum of the ε_i does not [3]. Curiously, the fact that the water molecule, H_2O , is also exceptional seems to have been overlooked. For water, the sum of the valence orbital energies decreases with decreasing bond angle so that the sum does predict that H_2O is non-linear, but this sum still has not reached a minimum at a 45° bond angle [8] so it can hardly be regarded as a reliable prediction of geometry.

In a previous paper [9] a generalized form of the self-consistent-field equation was derived. One special case of this generalization is the internally consistent SCF equation. This may be arrived at by noticing that, if the hamiltonian is partitioned into one and two body operators as

$$H = \sum_{i=1}^N [h(i) + (N-1)\alpha(i)] + \sum_{i < j}^N [g(i,j) - \alpha(i) - \alpha(j)], \quad (9)$$

$$h(i) = \frac{1}{2}V^2 - \sum_A Z_A r_{Ai}^{-1}, \quad (10)$$

$$g(i,j) = r_{ij}^{-1}, \quad (11)$$

where α is an arbitrary operator, then the Fock operator for a closed shell becomes

$$F_\alpha = F_0 + P\alpha P - Q\alpha Q + \text{Tr } \varrho \alpha \quad (12)$$

where F_0 is the usual Fock operator, P is the projector onto the occupied space, Q is the projector onto the virtual space, and ϱ is the charge density. If one insists that the one body part of H should be chosen to be F_α , i.e.

$$F_\alpha = h + (N - 1)\alpha, \quad (13)$$

then a partitioning of H commonly used in perturbation theory,

$$H = \sum F_\alpha(i) + \sum g_\alpha(i, j), \quad (14)$$

would match the partitioning used to obtain F .

This reasoning leads to an operator F_α whose matrix elements are easily expressed in terms of the canonical orbitals defined previously (3) as

$$F_{ij} = \langle \psi_i | F | \psi_j \rangle, \quad (15)$$

$$F_{ij} = (N - 2)^{-1} \{ (N - 1) \varepsilon_i \delta_{ij} - h_{ij} - V_{ee} \delta_{ij} \} + N^{-1} V_{NN} \delta_{ij} \quad (i, j \leq N/2), \quad (16)$$

$$F_{ij} = N^{-1} \{ (N - 1) \varepsilon_i \delta_{ij} + h_{ij} - V_{ee} \delta_{ij} \} + N^{-1} V_{NN} \delta_{ij} \quad (i, j > N/2), \quad (17)$$

$$F_{ij} = F_{ji} = 0 \quad (i \leq N/2, j > N/2), \quad (18)$$

$$V_{ee} = \sum_{i=1}^{N/2} (\varepsilon_i - h_{ii}), \quad (19)$$

$$V_{NN} = \text{nuclear-nuclear repulsion.} \quad (20)$$

Curiously, the orbital energies from

$$F_\alpha v_i = e_i v_i \quad (21)$$

satisfy

$$E_{\text{SCF}} = \sum_{i=1}^{N/2} n_i e_i. \quad (22)$$

So the sum of the orbital energies is the total energy in contrast to the conventional definitions. Also as was shown in the previous paper, the difference $e_i - e_j$ on the average is close to the excitation energy for transitions between valence orbitals.

Hence these orbital energies e_i would seem to have many of the properties attributed by Walsh to his orbital binding energies. Thus it was of some interest to calculate the e_i and to see whether they would behave in a reasonable manner as bond angles were varied. Reasonable behavior in this sense would mean behavior not too different from the ε_i or from Walsh's plots and not too much angle dependence in the e_i corresponding to 1s core orbitals.

Results

Calculations have been carried out using the polyatomic package of programs written by Langhoff and Elbert. Both the canonical (RHF) and internally consistent (ICSCF) orbitals were obtained. All calculations except that for CO₂

Table 1. The $1a_1^2 2a_1^2 1b_2^2 {}^1A_1$ state of BeH₂

	90	110	120	140	160	180	α_e
ICSCF							
$1a_1$	-5.1554	-5.1414	-5.1349	-5.1244	-5.1176	-5.1153	
$2a_1$	-1.3989	-1.3961	-1.3961	-1.3970	-1.3980	-1.3984	
$3a_1$	-1.0466	-1.0281	-1.0174	-0.9954	-0.9768	-0.9689	
$1b_1$	-0.9763	-0.9746	-0.9733	-0.9709	-0.9694	-0.9689	
$1b_2$	-1.2710	-1.3058	-1.3190	-1.3387	-1.3504	-1.3543	
$\Sigma_{\text{val}} \varepsilon$	-5.3398	-5.4038	-5.4302	-5.4714	-5.4968	-5.5054	180
E	-15.6508	-15.6866	-15.7001	-15.7201	-15.7320	-15.7359	180
Canonical							
$1a_1$	-4.7654	-4.7569	-4.7533	-4.7473	-4.7432	-4.7418	
$2a_1$	-0.5129	-0.5041	-0.5022	-0.5002	-0.4994	-0.4992	
$3a_1$	-0.0089	0.0067	0.0151	0.0319	0.0461	0.0526	
$1b_1$	0.0497	0.0507	0.0511	0.0519	0.0524	0.0526	
$1b_2$	-0.3582	-0.3940	-0.4081	-0.4293	-0.4419	-0.4460	
$\Sigma_{\text{val}} \varepsilon$	-1.7422	-1.7962	-1.8206	-1.8788	-1.8826	-1.8904	180
$\Sigma_{\text{all}} \varepsilon$	-11.2730	-11.3100	-11.3272	-11.3734	-11.3690	-11.3740	180

Table 2. The $1a_1^2 2a_1^2 1b_2^1 3a_1^1 {}^3B_2$ state of BeH₂

	90	110	120	140	160	180	α_e
ICSCF							
$1a_1$	-5.0953	-5.0912	-5.0902	-5.0907	-5.0939	-5.0968	
$2a_1$	-1.4080	-1.3942	-1.3889	-1.3802	-1.3737	-1.3709	
$3a_1$	-1.1999	-1.1808	-1.1701	-1.1473	-1.1246	-1.1119	
$1b_1$	-0.9443	-0.9445	-0.9444	-0.9442	-0.9442	-0.9442	
$1b_2$	-1.3734	-1.4102	-1.4226	-1.4395	-1.4487	-1.4518	
$\Sigma_{\text{val}} \varepsilon$	-5.3893	-5.3794	-5.3705	-5.3472	-5.3207	-5.3055	<90
E	-15.5799	-15.5618	-15.5511	-15.5288	-15.5085	-15.4990	<90
Canonical							
$1a_1$	-4.7572	-4.7571	-4.7581	-4.7617	-4.7676	-4.7720	
$2a_1$	-0.5608	-0.5435	-0.5372	-0.5279	-0.5229	-0.5219	
$3a_1$	-0.2820	-0.2664	-0.2575	-0.2375	-0.2164	-0.2040	
$1b_1$	0.0486	0.0480	0.0476	0.0465	0.0450	0.0440	
$1b_2$	-0.4835	-0.5193	-0.5324	-0.5519	-0.5648	-0.5704	
$\Sigma_{\text{val}} \varepsilon$	-1.8871	-1.8727	-1.8643	-1.8452	-1.8270	-1.8182	<90
$\Sigma_{\text{all}} \varepsilon$	-11.4015	-11.3869	-11.3805	-11.3686	-11.3622	-11.3622	<90

used contracted Gaussian lobe functions published by Whitten [10]. The calculation for CO₂ used a basis set based on Huzinaga's primitive Gaussians with the contraction optimized by Elbert. In order to lower the cost of this exploratory calculation, the same basis set and the same bond length was used for positive and negative ions and for all states of the neutral molecule. The scale factors for the hydrogen basis functions were taken from the work of Peyerimhoff *et al.* [7].

Table 3. The $1a_1^2 2a_1^2 1b_2^1 1b_1^1 {}^3A_2$ state of BeH₂

	90	110	120	140	160	180	α_e
ICSCF							
$1a_1$	-5.1248	-5.1132	-5.1082	-5.1003	-5.0953	-5.0937	
$2a_1$	-1.3868	-1.3781	-1.3756	-1.3725	-1.3711	-1.3707	
$3a_1$	-1.0114	-0.9960	-0.9870	-0.9682	-0.9513	-0.9438	
$1b_1$	-1.1281	-1.1245	-1.1227	-1.1197	-1.1180	-1.1175	
$1b_2$	-1.3625	-1.4044	-1.4196	-1.4416	-1.4541	-1.4582	
$\Sigma_{\text{val}} \varepsilon$	-5.2642	-5.2851	-5.2935	-5.3063	-5.3143	-5.3171	180
E	-15.5138	-15.5115	-15.5098	-15.5069	-15.5051	-15.5046	< 90
Canonical							
$1a_1$	-4.7850	-4.7786	-4.7760	-4.7720	-4.7693	-4.7684	
$2a_1$	-0.5482	-0.5346	-0.5303	-0.5246	-0.5216	-0.5206	
$3a_1$	-0.0093	0.0035	0.0106	0.0254	0.0386	0.0448	
$1b_1$	-0.2104	-0.2101	-0.2100	-0.2099	-0.2097	-0.2096	
$1b_2$	-0.4799	-0.5197	-0.5348	-0.5571	-0.5703	-0.5746	
$\Sigma_{\text{val}} \varepsilon$	-1.7867	-1.7990	-1.8054	-1.8162	-1.8232	-1.8254	180
$\Sigma_{\text{all}} \varepsilon$	-11.3567	-11.3562	-11.3574	-11.3602	-11.3618	-11.3622	180

Table 4. The $1a_1^2 2a_1^2 1b_2^2 {}^1A_1$ state of BH₂⁺

	90	110	120	140	160	180	α_e
ICSCF							
$1a_1$	-8.5547	-8.5482	-8.5444	-8.5373	-8.5327	-8.5311	
$2a_1$	-2.1651	-2.1545	-2.1512	-2.1472	-2.1450	-2.1443	
$3a_1$	-1.7140	-1.6940	-1.6826	-1.6596	-1.6416	-1.6346	
$1b_1$	-1.6393	-1.6393	-1.6385	-1.6366	-1.6352	-1.6346	
$1b_2$	-1.9424	-1.9850	-2.0016	-2.0271	-2.0423	-2.0475	
$\Sigma_{\text{val}} \varepsilon$	-8.2150	-8.2790	-8.3056	-8.3486	-8.3746	-8.3836	180
E	-25.3244	-25.3753	-25.3945	-25.4232	-25.4401	-25.4457	180
Canonical							
$1a_1$	-8.0901	-8.0881	-8.0868	-8.0847	-8.0833	-8.0829	
$2a_1$	-1.0299	-1.0151	-1.0103	-1.0043	-1.0009	-0.9999	
$3a_1$	-0.3324	-0.3101	-0.2978	-0.2736	-0.2542	-0.2466	
$1b_1$	-0.2465	-0.2468	-0.2467	-0.2466	-0.2466	-0.2466	
$1b_2$	-0.7904	-0.8334	-0.8511	-0.8792	-0.8962	-0.9021	
$\Sigma_{\text{val}} \varepsilon$	-3.6406	-3.6970	-3.7228	-3.7670	-3.7942	-3.8040	180
$\Sigma_{\text{all}} \varepsilon$	-19.8208	-19.8732	-19.8964	-19.9364	-19.9608	-19.9698	180

The bond length was held constant at its experimental equilibrium value as the bond angle was varied. This procedure is admittedly crude, but it should be sufficiently accurate to illustrate the behavior of the ICSCF method.

For all of the AH₂ systems studied [see Tables 1–25 and Figs. 1–23] the predicted geometry from E_{SCF} is in agreement with Walsh's rules. The six electron

Table 5. The $1a_1^2 2a_1^2 1b_2^2 3a_1^1 2A_1$ state of BH_2

	90	110	120	140	160	180	α_e
ICSCF							
$1a_1$	-8.3138	-8.3113	-8.3100	-8.3080	-8.3079	-8.3083	
$2a_1$	-1.9573	-1.9440	-1.9394	-1.9329	-1.9287	-1.9273	
$3a_1$	-1.6914	-1.6667	-1.6519	-1.6202	-1.5914	-1.5781	
$1b_1$	-1.4498	-1.4517	-1.4519	-1.4519	-1.4518	-1.4517	
$1b_2$	-1.7249	-1.7664	-1.7826	-1.8080	-1.8241	-1.8300	
$\Sigma_{\text{val}} \epsilon$	-9.0558	-9.0875	-9.0959	-9.1020	-9.0970	-9.0927	141
E	-25.6834	-25.7099	-25.7159	-25.7180	-25.7129	-25.7094	136
Canonical							
$1a_1$	-7.6310	-7.6274	-7.6266	-7.6265	-7.6286	-7.6302	
$2a_1$	-0.7005	-0.6796	-0.6725	-0.6630	-0.6585	-0.6577	
$3a_1$	-0.3935	-0.3677	-0.3536	-0.3234	-0.2968	-0.2840	
$1b_1$	0.0597	0.0605	0.0606	0.0602	0.0591	0.0584	
$1b_2$	-0.4409	-0.4809	-0.4975	-0.5249	-0.5433	-0.5506	
$\Sigma_{\text{val}} \epsilon$	-2.6763	-2.6887	-2.6936	-2.6992	-2.7004	-2.7006	180
$\Sigma_{\text{all}} \epsilon$	-17.9383	-17.9435	-17.9468	-17.9522	-17.9576	-17.9610	180

Table 6. The $1a_1^2 2a_1^2 1b_2^2 1b_1^1 2B_1$ state of BH_2

	90	110	120	140	160	180	α_e
ICSCF							
$1a_1$	-8.3307	-8.3234	-8.3198	-8.3135	-8.3097	-8.3083	
$2a_1$	-1.9448	-1.9356	-1.9329	-1.9297	-1.9279	-1.9273	
$3a_1$	-1.5365	-1.5154	-1.5033	-1.4789	-1.4594	-1.4517	
$1b_1$	-1.5870	-1.5856	-1.5842	-1.5812	-1.5789	-1.5781	
$1b_2$	-1.7260	-1.7682	-1.7846	-1.8098	-1.8249	-1.8300	
$\Sigma_{\text{val}} \epsilon$	-8.9286	-8.9932	-9.0192	-9.0602	-9.0845	-9.0927	180
E	-25.5901	-25.6401	-25.6590	-25.6872	-25.7038	-25.7094	180
Canonical							
$1a_1$	-7.6442	-7.6380	-7.6357	-7.6323	-7.6307	-7.6302	
$2a_1$	-0.6887	-0.6728	-0.6679	-0.6618	-0.6586	-0.6577	
$3a_1$	-0.0185	0.0031	0.0143	0.0358	0.0521	0.0584	
$1b_1$	-0.2891	-0.2867	-0.2859	-0.2847	-0.2842	-0.2840	
$1b_2$	-0.4426	-0.4843	-0.5014	-0.5284	-0.5449	-0.5506	
$\Sigma_{\text{val}} \epsilon$	-2.5517	-2.6009	-2.6245	-2.6651	-2.6912	-2.7006	180
$\Sigma_{\text{all}} \epsilon$	-17.8401	-17.8769	-17.8959	-17.9297	-17.9526	-17.9610	180

systems are found to be linear while the 7–10 electron systems are found to be bent. The calculated bond angles for bent molecules are within 10° of the known experimental angles which indicates that the RHF method with these basis sets is capable of quantitative as well as qualitative predictions.

Table 7. The $1a_1^2 2a_1^2 1b_2^2 3a_1^2 1A_1$ state of BH_2^-

	90	110	120	140	160	180	α_e
ICSCF							
$1a_1$	- 8.1501	- 8.1517	- 8.1529	- 8.1556	- 8.1587	- 8.1599	
$2a_1$	- 1.7687	- 1.7501	- 1.7423	- 1.7281	- 1.7163	- 1.7114	
$3a_1$	- 1.3728	- 1.3606	- 1.3537	- 1.3416	- 1.3341	- 1.3318	
$1b_1$	- 1.2699	- 1.2710	- 1.2710	- 1.2704	- 1.2698	- 1.2695	
$1b_2$	- 1.5270	- 1.5625	- 1.5758	- 1.5955	- 1.6071	- 1.6111	
$\Sigma_{\text{val}} \epsilon$	- 9.3370	- 9.3464	- 9.3436	- 9.3304	- 9.3150	- 9.3086	109
E	- 25.6373	- 25.6498	- 25.6494	- 25.6415	- 25.6322	- 25.6282	111
Canonical							
$1a_1$	- 7.3259	- 7.3272	- 7.3294	- 7.3354	- 7.3415	- 7.3441	
$2a_1$	- 0.4490	- 0.4256	- 0.4170	- 0.4035	- 0.3937	- 0.3899	
$3a_1$	0.0061	0.0232	0.0310	0.0436	0.0506	0.0526	
$1b_1$	0.2985	0.2990	0.2987	0.2976	0.2962	0.2956	
$1b_2$	- 0.1742	- 0.2138	- 0.2301	- 0.2567	- 0.2737	- 0.2798	
$\Sigma_{\text{val}} \epsilon$	- 1.2342	- 1.2324	- 1.2322	- 1.2332	- 1.2336	- 1.2342	< 90, 180
$\Sigma_{\text{all}} \epsilon$	- 15.8860	- 15.8868	- 15.8910	- 15.9040	- 15.9166	- 15.9224	180

Table 8. The $1a_1^2 2a_1^2 1b_2^2 1b_1 3a_1^2 3B_1$ state of BH_2^-

	90	110	120	140	160	180	α_e
ICSCF							
$1a_1$	- 8.1434	- 8.1418	- 8.1414	- 8.1414	- 8.1431	- 8.1442	
$2a_1$	- 1.7395	- 1.7259	- 1.7212	- 1.7143	- 1.7095	- 1.7077	
$3a_1$	- 1.4709	- 1.4489	- 1.4359	- 1.4089	- 1.3860	- 1.3764	
$1b_1$	- 1.3824	- 1.3834	- 1.3828	- 1.3805	- 1.3778	- 1.3764	
$1b_2$	- 1.5122	- 1.5504	- 1.5653	- 1.5884	- 1.6027	- 1.6077	
$\Sigma_{\text{val}} \epsilon$	- 9.3567	- 9.3849	- 9.3917	- 9.3948	- 9.3882	- 9.3836	136
E	- 25.6433	- 25.6686	- 25.6745	- 25.6775	- 25.2743	- 25.6720	140
Canonical							
$1a_1$	- 7.3210	- 7.3176	- 7.3176	- 7.3200	- 7.3249	- 7.3276	
$2a_1$	- 0.4232	- 0.4019	- 0.3951	- 0.3868	- 0.3834	- 0.3829	
$3a_1$	- 0.0995	- 0.0716	- 0.0567	- 0.0265	- 0.0006	0.0106	
$1b_1$	0.0145	0.0165	0.0165	0.0151	0.0122	0.0106	
$1b_2$	- 0.1620	- 0.2018	- 0.2184	- 0.2462	- 0.2653	- 0.2727	
$\Sigma_{\text{val}} \epsilon$	- 1.2554	- 1.2625	- 1.2672	- 1.2774	- 1.2858	- 1.2900	180
$\Sigma_{\text{all}} \epsilon$	- 15.8974	- 15.8977	- 15.9024	- 15.9174	- 15.9356	- 15.9452	180

The canonical orbital energy versus bond angle diagrams are quite similar to those reported and discussed at length by Peyerimhoff *et al.* [7]. Except for NH_2 , CH_2^- , and H_2O^+ the canonical orbital energies are in the order predicted by Walsh. This exception for NH_2 has been previously noted by Krauss [11]. The $2a_1$ orbital energy is seen to increase, not decrease as Walsh predicted, with

Table 9. The $1a_1^2 2a_1^2 1b_2^2 1b_1^2 {}^1A_1$ state of BH_2^-

	90	110	120	140	160	180	α_e
ICSCF							
$1a_1$	-8.1810	-8.1736	-8.1702	-8.1645	-8.1611	-8.1599	
$2a_1$	-1.7288	-1.7196	-1.7169	-1.7137	-1.7120	-1.7114	
$3a_1$	-1.3529	-1.3319	-1.3199	-1.2960	-1.2770	-1.2695	
$1b_1$	-1.3358	-1.3362	-1.3355	-1.3338	-1.3323	-1.3318	
$1b_2$	-1.5109	-1.5512	-1.5671	-1.5914	-1.6061	-1.6111	
$\Sigma_{\text{val}} \epsilon$	-9.1510	-9.2140	-9.2390	-9.2778	-9.3008	-9.3086	180
E	-25.5129	-25.5612	-25.5794	-25.6066	-25.6228	-25.6283	180
Canonical							
$1a_1$	-7.3623	-7.3540	-7.3511	-7.3469	-7.3448	-7.3441	
$2a_1$	-0.4239	-0.4066	-0.4012	-0.3945	-0.3909	-0.3899	
$3a_1$	0.2237	0.2444	0.2550	0.2749	0.2898	0.2956	
$1b_1$	0.0458	0.0489	0.0500	0.0516	0.0524	0.0526	
$1b_2$	-0.1751	-0.2157	-0.2323	-0.2584	-0.2744	-0.2798	
$\Sigma_{\text{val}} \epsilon$	-1.1064	-1.1468	-1.1670	-1.2026	-1.2258	-1.2342	180
$\Sigma_{\text{all}} \epsilon$	-15.8310	-15.8548	-15.8692	-15.8964	-15.9154	-15.9224	180

Table 10. The $1a_1^2 2a_1^2 1b_2^2 3a_1 {}^2A_1$ state of CH_2^+

	90	110	120	140	160	180	α_e
ICSCF							
$1a_1$	-12.6067	-12.6054	-12.6036	-12.5990	-12.5948	-12.5928	
$2a_1$	-2.8631	-2.8494	-2.8451	-2.8400	-2.8382	-2.8382	
$3a_1$	-2.5128	-2.4822	-2.4648	-2.4288	-2.3971	-2.3829	
$1b_1$	-2.2478	-2.2515	-2.2527	-2.2545	-2.2560	-2.2566	
$1b_2$	-2.5163	-2.5651	-2.5849	-2.6168	-2.6380	-2.6461	
$\Sigma_{\text{val}} \epsilon$	-13.2716	-13.3112	-13.3248	-13.3424	-13.3495	-13.3515	180
E	-38.4852	-38.5219	-38.5320	-38.5403	-38.5391	-38.5372	147
Canonical							
$1a_1$	-11.7566	-11.7515	-11.7482	-11.7406	-11.7329	-11.7293	
$2a_1$	-1.2843	-1.2631	-1.2549	-1.2423	-1.2341	-1.2314	
$3a_1$	-0.9302	-0.9009	-0.8847	-0.8515	-0.8223	-0.8093	
$1b_1$	-0.3030	-0.3018	-0.3009	-0.2990	-0.2971	-0.2962	
$1b_2$	-0.9196	-0.9606	-0.9775	-1.0040	-1.0199	-1.0255	
$\Sigma_{\text{val}} \epsilon$	-5.3380	-5.3483	-5.3495	-5.3441	-5.3303	-5.3231	114
$\Sigma_{\text{all}} \epsilon$	-28.8512	-28.8513	-28.8459	-28.8253	-28.7961	-28.7817	101

increase in bond angle, but this result has also been noted and explained previously [7]. For the most part, the change of the $3a_1$ orbital energy with bond angle is less than Walsh predicted, and the change of the $1b_1$ energy is somewhat greater than he expected (see Refs. [3, 7] for a detailed discussion). Figs. 19, 21 for the 2A_1 states of H_2O^+ and NH_2 even show the crossing of the $3a_1$ and $1b_2$ energies

Table 11. The $1a_1^2 2a_1^2 1b_2^2 1b_1^- {}^2B_1$ state of CH_2^+

	90	110	120	140	160	180	α_e
ICSCF							
$1a_1$	-12.6060	-12.6031	-12.6010	-12.5968	-12.5939	-12.5928	
$2a_1$	-2.8592	-2.8487	-2.8454	-2.8412	-2.8389	-2.8382	
$3a_1$	-2.3479	-2.3225	-2.3091	-2.2833	-2.2640	-2.2566	
$1b_1$	-2.3876	-2.3874	-2.3866	-2.3848	-2.3834	-2.3829	
$1b_2$	-2.5295	-2.5764	-2.5949	-2.6283	-2.6403	-2.6461	
$\Sigma_{\text{val}} \epsilon$	-13.1650	-13.2376	-13.2672	-13.3138	-13.3418	-13.3515	180
E	-38.3770	-38.4438	-38.4693	-38.5074	-38.5297	-38.5372	180
Canonical							
$1a_1$	-11.7375	-11.7354	-11.7341	-11.7317	-11.7299	-11.7293	
$2a_1$	-1.2622	-1.2481	-1.2432	-1.2365	-1.2326	-1.2314	
$3a_1$	-0.4026	-0.3728	-0.3574	-0.3280	-0.3051	-0.2962	
$1b_1$	-0.8110	-0.8110	-0.8107	-0.8100	-0.8094	-0.8093	
$1b_2$	-0.9113	-0.9551	-0.9733	-1.0020	-1.0194	-1.0255	
$\Sigma_{\text{val}} \epsilon$	-5.1580	-5.2174	-5.2437	-5.2870	-5.3134	-5.3231	180
$\Sigma_{\text{all}} \epsilon$	-28.6330	-28.6882	-28.7119	-28.7504	-28.7732	-28.7817	180

Table 12. The $1a_1^2 2a_1^2 1b_2^2 3a_1^- {}^1A_1$ state of CH_2

	90	110	120	140	160	180	α_e
ICSCF							
$1a_1$	-12.3671	-12.3560	-12.3647	-12.3614	-12.3587	-12.3574	
$2a_1$	-2.6426	-2.6244	-2.6171	-2.6039	-2.5930	-2.5885	
$3a_1$	-2.1145	-2.0954	-2.0857	-2.0689	-2.0590	-2.0560	
$1b_1$	-2.0204	-2.0231	-2.0240	-2.0252	-2.0260	-2.0262	
$1b_2$	-2.2853	-2.3311	-2.3490	-2.3768	-2.3938	-2.3996	
$\Sigma_{\text{val}} \epsilon$	-14.0848	-14.1018	-14.1036	-14.0992	-14.0916	-14.0882	116
E	-38.8190	-38.8336	-38.8328	-38.8221	-38.8089	-38.8033	114
Canonical							
$1a_1$	-11.2884	-11.2834	-11.2805	-11.2744	-11.2695	-11.2674	
$2a_1$	-0.9273	-0.9027	-0.8923	-0.8737	-0.8589	-0.8531	
$3a_1$	-0.3854	-0.3616	-0.3501	-0.3303	-0.3179	-0.3141	
$1b_1$	0.0519	0.0535	0.0544	0.0559	0.0570	0.0575	
$1b_2$	-0.5370	-0.5778	-0.5941	-0.6192	-0.6340	-0.6391	
$\Sigma_{\text{val}} \epsilon$	-3.6994	-3.6842	-3.6730	-3.6464	-3.6216	-3.6126	< 90
$\Sigma_{\text{all}} \epsilon$	-26.2762	-26.2510	-26.2340	-26.1952	-26.1606	-26.1474	< 90

as predicted by Walsh. Because the RHF self-consistent-field procedure treats virtual orbitals in an unsatisfactory manner, the energy assigned to an orbital changes drastically depending on whether it is occupied or empty. Thus, in contrast to Hückel theory and Walsh's reasoning, the canonical orbital energy plots change appearance not only between molecules but also from state to state of the same molecule.

Table 13. The $1a_1^2 2a_1^2 1b_2^2 3a_1$ 3B_1 state of CH₂

	90	110	120	140	160	180	α_e
ICSCF							
$1a_1$	-12.3409	-12.3391	-12.3377	-12.3346	-12.3325	-12.3316	
$2a_1$	-2.6113	-2.5980	-2.5936	-2.5877	-2.5844	-2.5836	
$3a_1$	-2.2507	-2.2203	-2.2032	-2.1680	-2.1371	-2.1233	
$1b_1$	-2.1183	-2.1207	-2.1213	-2.1221	-2.1229	-2.1233	
$1b_2$	-2.2758	-2.3224	-2.3410	-2.3704	-2.3894	-2.3964	
$\Sigma_{\text{val}} \varepsilon$	-14.1432	-14.1818	-14.1937	-14.2063	-14.2076	-14.2066	161
E	-38.8250	-38.8600	-38.8692	-38.8755	-38.8726	-38.8698	143
Canonical							
$1a_1$	-11.2562	-11.2510	-11.2487	-11.2443	-11.2411	-11.2397	
$2a_1$	-0.8874	-0.8675	-0.8603	-0.8500	-0.8440	-0.8424	
$3a_1$	-0.5085	-0.4752	-0.4576	-0.4221	-0.3911	-0.3771	
$1b_1$	-0.3842	-0.3818	-0.3807	-0.3789	-0.3776	-0.3771	
$1b_2$	-0.5170	-0.5591	-0.5765	-0.6043	-0.6219	-0.6284	
$\Sigma_{\text{val}} \varepsilon$	-3.7015	-3.7102	-3.7119	-3.7096	-3.7005	-3.6958	123
$\Sigma_{\text{all}} \varepsilon$	-26.2139	-26.2122	-26.2093	-26.1982	-26.1827	-26.1752	< 90

Table 14. The $1a_1^2 2a_1^2 1b_2^2 1b_1^2$ 1A_1 state of CH₂

	90	110	120	140	160	180	α_e
ICSCF							
$1a_1$	-12.3728	-12.3688	-12.3659	-12.3614	-12.3585	-12.3574	
$2a_1$	-2.6073	-2.5977	-2.5948	-2.5911	-2.5891	-2.5885	
$3a_1$	-2.1252	-2.0980	-2.0836	-2.0558	-2.0345	-2.0262	
$1b_1$	-2.0580	-2.0588	-2.0584	-2.0573	-2.0564	-2.0560	
$1b_2$	-2.2849	-2.3312	-2.3494	-2.3773	-2.3940	-2.3996	
$\Sigma_{\text{val}} \varepsilon$	-13.9004	-13.9754	-14.0052	-14.0514	-14.0790	-14.0882	180
E	-38.6459	-38.7119	-38.7369	-38.7742	-38.7960	-38.8033	180
Canonical							
$1a_1$	-11.2824	-11.2766	-11.2742	-11.2704	-11.2682	-11.2674	
$2a_1$	-0.8849	-0.8698	-0.8648	-0.8580	-0.8542	-0.8531	
$3a_1$	-0.0459	-0.0161	-0.0011	0.0273	0.0491	0.0575	
$1b_1$	-0.3195	-0.3175	-0.3166	-0.3152	-0.3143	-0.3141	
$1b_2$	-0.5270	-0.5702	-0.5880	-0.6161	-0.6331	-0.6391	
$\Sigma_{\text{val}} \varepsilon$	-3.4628	-3.5150	-3.5388	-3.5786	-3.6032	-3.6126	180
$\Sigma_{\text{all}} \varepsilon$	-26.0276	-26.0682	-26.0872	-26.1194	-26.1396	-26.1474	180

For the 2, 4, and 6 valence electron molecules (lowest singlet state), BeH₂, BH₂⁺, BH₂⁻, it was claimed [7] that the sum of the valence orbital ε_i correlated correctly with the geometry. The present results agree with the claim except that the orbital energy sum seems to predict too small a bond angle. Also as in that study [7], this correlation of geometry and the sum of the ε_i was not found to hold for the 6 electron system 1A_1 NH₂⁺. Examination of the 25 AH₂ results

Table 15. The $1a_1^2 2a_1^2 1b_2^2 3a_1^2 1b_1$ state of CH_2^-

	90	110	120	140	160	180	α_e
ICSCF							
$1a_1$	-12.1394	-12.1404	-12.1406	-12.1411	-12.1418	-12.1419	
$2a_1$	-2.3931	-2.3746	-2.3671	-2.3536	-2.3424	-2.3377	
$3a_1$	-1.8800	-1.8615	-1.8518	-1.8345	-1.8237	-1.8203	
$1b_1$	-1.8801	-1.8817	-1.8819	-1.8820	-1.8818	-1.8817	
$1b_2$	-2.0500	-2.0915	-2.1075	-2.1318	-2.1464	-2.1513	
$\Sigma_{\text{val}} \varepsilon$	-14.5263	-14.5369	-14.5347	-14.5218	-14.5068	-14.5003	110
E	-38.8051	-38.8177	-38.8161	-38.8041	-38.7901	-38.7842	112
Canonical							
$1a_1$	-10.8920	-10.8893	-10.8888	-10.8887	-10.8895	-10.8898	
$2a_1$	-0.5805	-0.5563	-0.5468	-0.5310	-0.5190	-0.5142	
$3a_1$	-0.0373	-0.0116	0.0005	0.0210	0.0338	0.0378	
$1b_1$	-0.0339	-0.0309	-0.0300	-0.0290	-0.0287	-0.0286	
$1b_2$	-0.1909	-0.2323	-0.2492	-0.2758	-0.2923	-0.2981	
$\Sigma_{\text{val}} \varepsilon$	-1.6513	-1.6313	-1.6210	-1.6006	-1.5837	-1.5776	< 90
$\Sigma_{\text{all}} \varepsilon$	-23.4353	-23.4099	-23.3986	-23.3780	-23.3627	-23.3572	< 90

Table 16. The $1a_1^2 2a_1^2 1b_2^2 3a_1 1b_1^2$ state of CH_2^-

	90	110	120	140	160	180	α_e
ICSCF							
$1a_1$	-12.1463	-12.1446	-12.1437	-12.1421	-12.1418	-12.1419	
$2a_1$	-2.3676	-2.3542	-2.3497	-2.3432	-2.3391	-2.3377	
$3a_1$	-2.0011	-1.9719	-1.9556	-1.9224	-1.8940	-1.8817	
$1b_1$	-1.8168	-1.8194	-1.8199	-1.8203	-1.8203	-1.8203	
$1b_2$	-2.0405	-2.0840	-2.1013	-2.1282	-2.1452	-2.1513	
$\Sigma_{\text{val}} \varepsilon$	-14.4509	-14.4871	-14.4974	-14.5062	-14.5032	-14.5003	145
E	-38.7432	-38.7762	-38.7846	-37.7901	-38.7869	-38.7842	143
Canonical							
$1a_1$	-10.9004	-10.8943	-10.8922	-10.8898	-10.8895	-10.8898	
$2a_1$	-0.5585	-0.5375	-0.5303	-0.5205	-0.5154	-0.5142	
$3a_1$	-0.1659	-0.1297	-0.1111	-0.0742	-0.0426	-0.0286	
$1b_1$	0.0321	0.0356	0.0367	0.0379	0.0380	0.0378	
$1b_2$	-0.1864	-0.2279	-0.2452	-0.2731	-0.2913	-0.2981	
$\Sigma_{\text{val}} \varepsilon$	-1.5915	-1.5893	-1.5889	-1.5856	-1.5800	-1.5776	< 90
$\Sigma_{\text{all}} \varepsilon$	-23.3923	-23.3779	-23.3733	-23.3652	-23.3590	-23.3572	< 90

presented here show that in seven cases the sum of the valence orbital ε_i correctly predicted the linear geometry, and in one case it satisfactorily predicted the non-linear geometry. In three cases it predicted the molecule to be linear when it wasn't. But the most consistent trend was shown in 14 out of the 25 cases where the predicted bond angle was significantly less than that shown by E_{SCF} . This error was not due to the effect of the core orbitals since inclusion of them in the sum only made the quantitative predictions worse.

Table 17. The $1a_1^2 2a_1^2 1b_2^2 3a_1^2 1A_1$ state of NH_2^+

	90	110	120	140	160	180	α_e
ICSCF							
$1a_1$	-17.5004	-17.4975	-17.4946	-17.4873	-17.4809	-17.4782	
$2a_1$	-3.7312	-3.7142	-3.7075	-3.6965	-3.6881	-3.6849	
$3a_1$	-3.0756	-3.0537	-3.0432	-3.0251	-3.0137	-3.0100	
$1b_1$	-2.9910	-2.9957	-2.9975	-3.0001	-3.0020	-3.0025	
$1b_2$	-3.2291	-3.2814	-3.3026	-3.3364	-3.3578	-3.3653	
$\Sigma_{\text{val}} \varepsilon$	-20.0718	-20.0986	-20.1066	-20.1160	-20.1192	-20.1204	180
E	-55.0726	-55.0935	-55.0958	-55.0905	-55.0811	-55.0767	116
Canonical							
$1a_1$	-16.1329	-16.1208	-16.1133	-16.0972	-16.0836	-16.0783	
$2a_1$	-1.5835	-1.5564	-1.5439	-1.5215	-1.5040	-1.4974	
$3a_1$	-0.9448	-0.9179	-0.9047	-0.8816	-0.8660	-0.8607	
$1b_1$	-0.3734	-0.3689	-0.3661	-0.3605	-0.3557	-0.3538	
$1b_2$	-1.0614	-1.0981	-1.1125	-1.1344	-1.1464	-1.1504	
$\Sigma_{\text{val}} \varepsilon$	-7.1794	-7.1448	-7.1222	-7.0750	-7.0328	-7.0170	< 90
$\Sigma_{\text{all}} \varepsilon$	-39.4452	-39.3864	-39.3488	-39.2694	-39.2000	-39.1736	< 90

Table 18. The $1a_1^2 2a_1^2 1b_2^2 3a_1^1 1b_1^1 3B_1$ state of NH_2^+

	90	110	120	140	160	180	α_e
ICSCF							
$1a_1$	-17.4585	-17.4584	-17.4572	-17.4531	-17.4491	-17.4472	
$2a_1$	-3.6999	-3.6874	-3.6835	-3.6786	-3.6766	-3.6764	
$3a_1$	-3.2364	-3.2008	-3.1820	-3.1448	-3.1142	-3.1013	
$1b_1$	-3.0906	-3.0947	-3.0961	-3.0984	-3.1004	-3.1013	
$1b_2$	-3.2235	-3.2747	-3.2956	-3.3291	-3.3509	-3.3589	
$\Sigma_{\text{val}} \varepsilon$	-20.1738	-20.2197	-20.2363	-20.2586	-20.2696	-20.2732	180
E	-55.0908	-55.1367	-55.1505	-55.1648	-55.1679	-55.1676	168
Canonical							
$1a_1$	-16.0787	-16.0732	-16.0694	-16.0609	-16.0524	-16.0486	
$2a_1$	-1.5345	-1.5159	-1.5086	-1.4969	-1.4889	-1.4863	
$3a_1$	-1.0772	-1.0419	-1.0235	-0.9884	-0.9596	-0.9476	
$1b_1$	-0.9622	-0.9597	-0.9579	-0.9537	-0.9495	-0.9476	
$1b_2$	-1.0344	-1.0751	-1.0918	-1.1182	-1.1337	-1.1390	
$\Sigma_{\text{val}} \varepsilon$	-7.1772	-7.1836	-7.1822	-7.1723	-7.1543	-7.1470	110
$\Sigma_{\text{all}} \varepsilon$	-39.3346	-39.3300	-39.3210	-39.2941	-39.2591	-39.2442	< 90

From the limited data shown here, it would appear possible in some of these 14 cases that the sum of the ε_i might show a minimum, and therefore better correlation with the total energy, if calculations were done at some angles between 90° and 110° . However, other work by Krauss [11] reports decreases in the sum of the ε_i at 5° intervals over parts of this range for 1A_1 CH_2 , 2B_1 NH_2 , and 2B_1 H_2O^+ which seem to be linear with respect to decrease in angle.

Table 19. The $1a_1^2 2a_1^2 1b_2^2 1b_1^2 A_1$ state of NH_2^+

	90	110	120	140	160	180	α_e
ICSCF							
$1a_1$	-17.4819	-17.4825	-17.4819	-17.4802	-17.4788	-17.4782	
$2a_1$	-3.7056	-3.6956	-3.6923	-3.6880	-3.6856	-3.6849	
$3a_1$	-3.1020	-3.0722	-3.0574	-3.0299	-3.0100	-3.0025	
$1b_1$	-3.0089	-3.0107	-3.0109	-3.0105	-3.0102	-3.0100	
$1b_2$	-3.2441	-3.2927	-3.3118	-3.3414	-3.3592	-3.3653	
$\Sigma_{\text{val}} \epsilon$	-19.9172	-19.9966	-20.0300	-20.0798	-20.1100	-20.1204	180
E	-54.8810	-54.9627	-54.9939	-55.0402	-55.0676	-55.0767	180
Canonical							
$1a_1$	-16.0832	-16.0824	-16.0816	-16.0800	-16.0787	-16.0783	
$2a_1$	-1.5263	-1.5137	-1.5090	-1.5026	-1.4986	-1.4974	
$3a_1$	-0.4793	-0.4422	-0.4239	-0.3899	-0.3638	-0.3538	
$1b_1$	-0.8617	-0.8620	-0.8618	-0.8613	-0.8608	-0.8607	
$1b_2$	-1.0374	-1.0804	-1.0982	-1.1270	-1.1443	-1.1504	
$\Sigma_{\text{val}} \epsilon$	-6.8508	-6.9122	-6.9380	-6.9818	-7.0048	-7.0170	180
$\Sigma_{\text{all}} \epsilon$	-39.0172	-39.0770	-39.1012	-39.1418	-39.1622	-39.1736	180

Table 20. The $1a_1^2 2a_1^2 1b_2^2 3a_1^2 1b_1^2 B_1$ state of NH_2

	90	110	120	140	160	180	α_e
ICSCF							
$1a_1$	-17.1816	-17.1801	-17.1783	-17.1733	-17.1688	-17.1668	
$2a_1$	-3.4327	-3.4159	-3.4092	-3.3979	-3.3887	-3.3850	
$3a_1$	-2.7931	-2.7678	-2.7553	-2.7334	-2.7191	-2.7143	
$1b_1$	-2.7910	-2.7944	-2.7957	-2.7979	-2.7996	-2.8003	
$1b_2$	-2.9492	-2.9993	-3.0192	-3.0507	-3.0704	-3.0773	
$\Sigma_{\text{val}} \epsilon$	-21.1410	-21.1604	-21.1631	-21.1619	-21.1560	-21.1535	127
E	-55.5043	-55.5204	-55.5198	-55.5083	-55.4936	-55.4872	114
Canonical							
$1a_1$	-15.5763	-15.5684	-15.5634	-15.5526	-15.5433	-15.5395	
$2a_1$	-1.1295	-1.1059	-1.0954	-1.0765	-1.0613	-1.0553	
$3a_1$	-0.4805	-0.4502	-0.4356	-0.4099	-0.3928	-0.3871	
$1b_1$	-0.5004	-0.4953	-0.4922	-0.4857	-0.4801	-0.4778	
$1b_2$	-0.6019	-0.6424	-0.6584	-0.6829	-0.6969	-0.7017	
$\Sigma_{\text{val}} \epsilon$	-4.9242	-4.8923	-4.8710	-4.8243	-4.7821	-4.7660	< 90
$\Sigma_{\text{all}} \epsilon$	-36.0768	-36.0291	-35.9978	-35.9295	-35.8687	-35.8450	< 90

This tendency to produce bond angles systematically too small can be predicted from Eq. (7). If the hydrogens carry any net positive charge, $V_N - V_e$ will tend to increase as the bond angle is decreased and the charges are brought closer together. Hence $\Sigma 2e_i$ must be systematically wrong in just the opposite direction so the two quantities will give E_{SCF} when added together. The few cases where the bond

Table 21. The $1a_1^2 2a_1^2 1b_2^2 3a_1 1b_1^2 {}^2A_1$ state of NH₂

	90	110	120	140	160	180	α_e
ICSCF							
$1a_1$	-17.1777	-17.1767	-17.1753	-17.1717	-17.1684	-17.1668	
$2a_1$	-3.4102	-3.3980	-3.3939	-3.3885	-3.3856	-3.3850	
$3a_1$	-2.9394	-2.9031	-2.8839	-2.8459	-2.8140	-2.8003	
$1b_1$	-2.7051	-2.7086	-2.7098	-2.7118	-2.7135	-2.7143	
$1b_2$	-2.9476	-2.9974	-3.0174	-3.0492	-3.0698	-3.0773	
$\Sigma_{\text{val}} \epsilon$	-21.0652	-21.1043	-21.1261	-21.1449	-21.1518	-21.1535	180
E	-55.4204	-55.4644	-55.4769	-55.4884	-55.4887	-55.4872	153
Canonical							
$1a_1$	-15.5654	-15.5594	-15.5561	-15.5489	-15.5424	-15.5395	
$2a_1$	-1.0993	-1.0815	-1.0747	-1.0643	-1.0575	-1.0553	
$3a_1$	-0.6195	-0.5804	-0.5607	-0.5226	-0.4911	-0.4778	
$1b_1$	-0.3993	-0.3965	-0.3949	-0.3916	-0.3885	-0.3871	
$1b_2$	-0.5928	-0.6349	-0.6521	-0.6795	-0.6960	-0.7017	
$\Sigma_{\text{val}} \epsilon$	-4.8023	-4.8062	-4.8041	-4.7934	-4.7751	-4.7660	110
$\Sigma_{\text{all}} \epsilon$	-35.9331	-35.9250	-35.9163	-35.8913	-35.8599	-35.8450	< 90

Table 22. The $1a_1^2 2a_1^2 1b_2^2 3a_1^2 1b_1^2 {}^1A_1$ state of NH₂

	90	110	120	140	160	180	α_e
ICSCF							
$1a_1$	-16.9322	-16.9319	-16.9312	-16.9289	-16.9269	-16.9259	
$2a_1$	-3.1503	-3.1335	-3.1270	-3.1150	-3.1052	-3.1010	
$3a_1$	-2.5212	-2.4951	-2.4819	-2.4581	-2.4420	-2.4366	
$1b_1$	-2.4294	-2.4323	-2.4333	-2.4350	-2.4362	-2.4366	
$1b_2$	-2.6845	-2.7310	-2.7494	-2.7779	-2.7957	-2.8019	
$\Sigma_{\text{val}} \epsilon$	-21.5708	-21.5838	-21.5832	-21.5720	-21.5582	-21.5522	115
E	-55.4353	-55.4478	-55.4452	-55.4298	-55.4118	-55.4040	110
Canonical							
$1a_1$	-15.1475	-15.1409	-15.1376	-15.1308	-15.1251	-15.1227	
$2a_1$	-0.7380	-0.7144	-0.7046	-0.6871	-0.6729	-0.6670	
$3a_1$	-0.0865	-0.0528	-0.0370	-0.0092	0.0093	0.0155	
$1b_1$	-0.0033	0.0019	0.0044	0.0093	0.0136	0.0155	
$1b_2$	-0.2095	-0.2511	-0.2677	-0.2933	-0.3082	-0.3131	
$\Sigma_{\text{val}} \epsilon$	-2.0746	-2.0404	-2.0274	-1.9978	-2.0080	-2.0222	< 90, 180
$\Sigma_{\text{all}} \epsilon$	-32.3696	-32.3222	-32.3010	-32.2594	-32.2582	-32.2676	< 90

angle was overestimated were the cases where one would expect the hydrogens to carry a net negative charge, and the bulk of the cases such as H₂O where the bond angle was underestimated were just those cases where the hydrogens were expected to carry a net positive charge.

Table 23. The $1a_1^2 2a_1^2 1b_2^2 3a_1^2 1b_1 {}^2B_1 \text{H}_2\text{O}^+$

	90	110	120	140	160	180	α_e
ICSCF							
$1a_1$	-23.1359	-23.1329	-23.1300	-23.1226	-23.1159	-23.1131	
$2a_1$	-4.7054	-4.6913	-4.6857	-4.6766	-4.6703	-4.6679	
$3a_1$	-3.9189	-3.8909	-3.8780	-3.8558	-3.8410	-3.8360	
$1b_1$	-3.9352	-3.9401	-3.9422	-3.9458	-3.9484	-3.9495	
$1b_2$	-4.0531	-4.1071	-4.1290	-4.1637	-4.1856	-4.1932	
$\Sigma_{\text{val}} \epsilon$	-29.2900	-29.3187	-29.3276	-29.3380	-29.3422	-29.3437	180
E	-75.5617	-75.5844	-75.5875	-75.5832	-75.5741	-75.5698	119
Canonical							
$1a_1$	-21.1317	-21.1184	-21.1101	-21.0919	-21.0764	-21.0702	
$2a_1$	-1.8651	-1.8412	-1.8296	-1.8080	-1.7914	-1.7850	
$3a_1$	-1.0931	-1.0615	-1.0460	-1.0185	-0.9996	-0.9929	
$1b_1$	-1.1444	-1.1366	-1.1316	-1.1210	-1.1120	-1.1084	
$1b_2$	-1.1850	-1.2213	-1.2354	-1.2561	-1.2674	-1.2708	
$\Sigma_{\text{val}} \epsilon$	-9.4308	-9.3846	-9.3536	-9.2862	-9.2288	-9.2058	< 90
$\Sigma_{\text{all}} \epsilon$	-51.6942	-51.6214	-51.5738	-51.4700	-51.3816	-51.3462	< 90

Table 24. The $1a_1^2 2a_1^2 1b_2^2 3a_1^1 1b_1^2 {}^2A_1$ state of H_2O^+

	90	110	120	140	160	180	α_e
ICSCF							
$1a_1$	-23.1235	-23.1237	-23.1226	-23.1190	-23.1149	-23.1131	
$2a_1$	-4.6880	-4.6778	-4.6744	-4.6700	-4.6683	-4.6679	
$3a_1$	-4.0868	-4.0472	-4.0274	-3.9903	-3.9611	-3.9495	
$1b_1$	-3.8232	-3.8278	-3.8296	-3.8326	-3.8350	-3.8360	
$1b_2$	-4.0572	-4.1092	-4.1305	-4.1640	-4.1856	-4.1932	
$\Sigma_{\text{val}} \epsilon$	-29.2236	-29.2768	-29.2964	-29.3235	-29.3389	-29.3437	180
E	-75.4704	-75.5243	-75.5416	-75.5615	-75.5685	-75.5698	180
Canonical							
$1a_1$	-21.1034	-21.0977	-21.0935	-21.0837	-21.0743	-21.0702	
$2a_1$	-1.8293	-1.8141	-1.8074	-1.7958	-1.7879	-1.7850	
$3a_1$	-1.2402	-1.2019	-1.1827	-1.1469	-1.1193	-1.1084	
$1b_1$	-1.0096	-1.0070	-1.0049	-1.0000	-0.9950	-0.9929	
$1b_2$	-1.1694	-1.2097	-1.2261	-1.2514	-1.2661	-1.2708	
$\Sigma_{\text{val}} \epsilon$	-9.2568	-9.2635	-9.2595	-9.2413	-9.2173	-9.2058	110
$\Sigma_{\text{all}} \epsilon$	-51.4636	-51.4589	-51.4465	-51.3817	-51.3659	-51.3462	< 90

The ICSCF results are somewhat superior to the canonical results. The $1a_1$ ICSCF orbital energy changes with angle, on the average, only half as much as does the RHF ϵ_i (but notice later that wherever the ICSCF makes the wrong prediction, it is, by definition, due to the change of the $1a_1$ energy). Except for

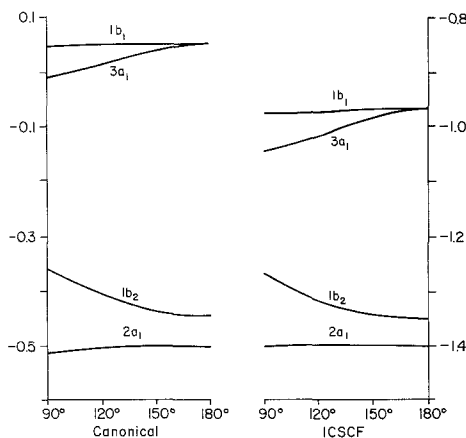
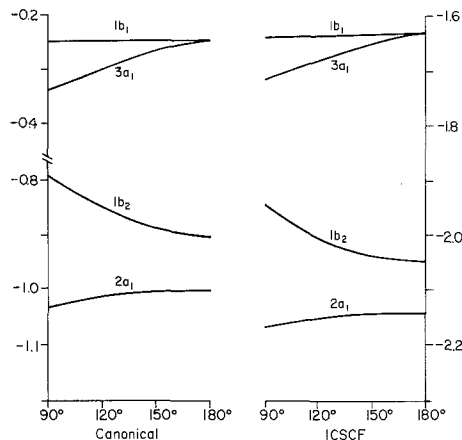
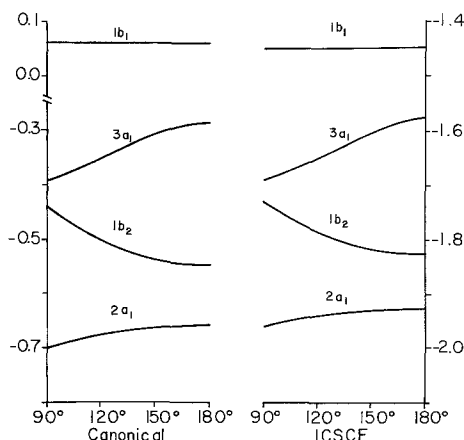
Table 25. The $1a_1^2 2a_1^2 1b_2^2 3a_1^2 1b_1^{2,1} A_1$ state of H₂O

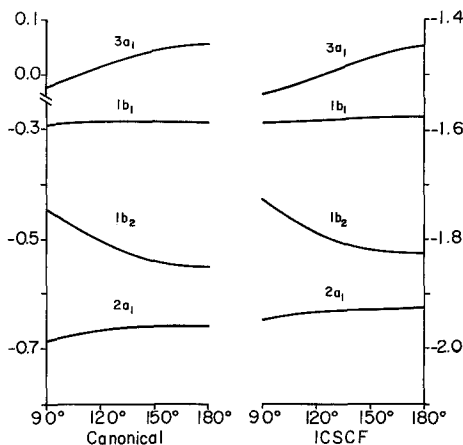
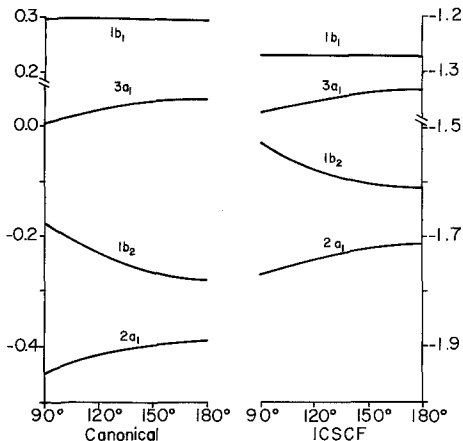
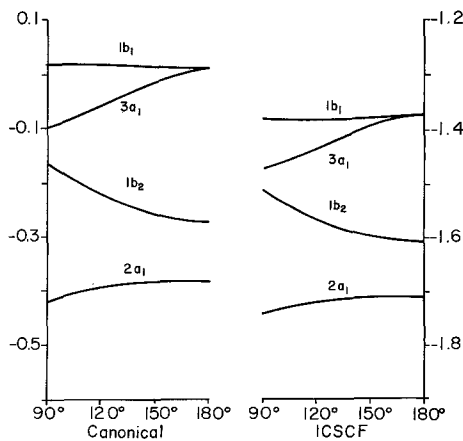
	90	110	120	140	160	180	α_e
ICSCF							
$1a_1$	-22.8025	-22.8010	-22.7975	-22.7911	-22.7849	-22.7823	
$2a_1$	-4.3688	-4.3548	-4.3493	-4.3400	-4.3330	-4.3301	
$3a_1$	-3.5968	-3.5648	-3.5497	-3.5230	-3.5048	-3.4985	
$1b_1$	-3.4855	-3.4896	-3.4914	-3.4948	-3.4974	-3.4985	
$1b_2$	-3.7358	-3.7887	-3.8098	-3.8429	-3.8638	-3.8711	
$\Sigma_{\text{val}} \varepsilon$	-30.3738	-30.3958	-30.4004	-30.4014	-30.3980	-30.3964	135
E	-75.9787	-75.9959	-75.9954	-75.9835	-75.9678	-75.9608	115
Canonical							
$1a_1$	-20.5650	-20.5548	-20.5481	-20.5332	-20.5199	-20.5144	
$2a_1$	-1.3761	-1.3552	-1.3452	-1.3262	-1.3110	-1.3048	
$3a_1$	-0.5928	-0.5576	-0.5405	-0.5102	-0.4894	-0.4821	
$1b_1$	-0.5117	-0.5055	-0.5016	-0.4930	-0.4853	-0.4821	
$1b_2$	-0.6891	-0.7291	-0.7447	-0.7677	-0.7803	-0.7843	
$\Sigma_{\text{val}} \varepsilon$	-6.3394	-6.2948	-6.2640	-6.1942	-6.1320	-6.1066	< 90
$\Sigma_{\text{all}} \varepsilon$	-47.4694	-47.4044	-47.3602	-47.2606	-47.1718	-47.1354	< 90

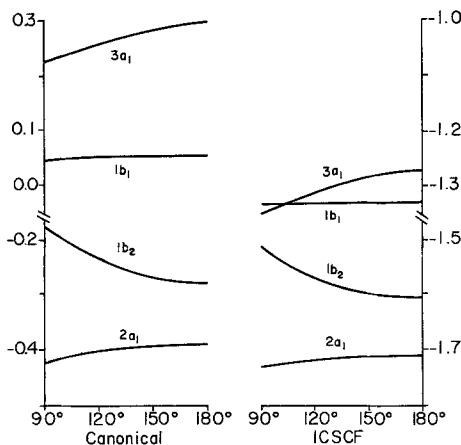
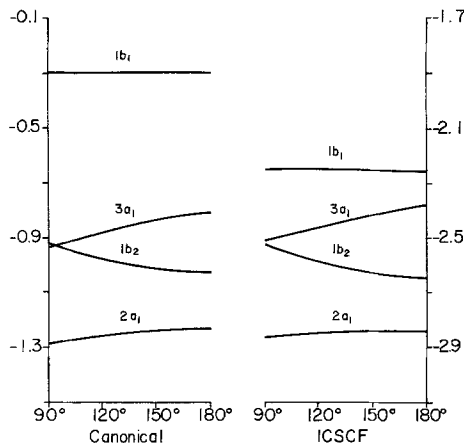
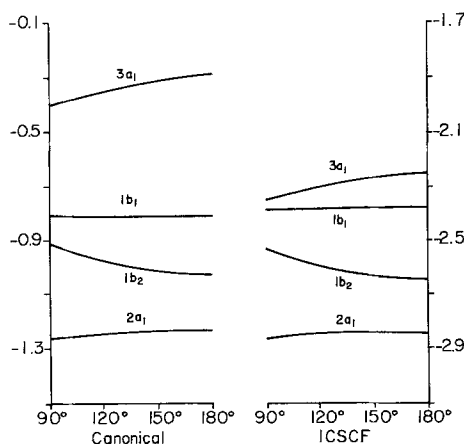
BeH₂, e_{1a} changes less than 15 kcal (and usually only half that amount) as the bond angle varies from 90–180°. The other orbital energy curves are generally similar to the RHF results. The $2a_1$ orbital energy still has a positive slope, but perhaps a little less steep. The $1b_2$ and $3a_1$ orbital energy curves are nearly identical in shape to the canonical result. The $1b_1$ curves are generally even flatter than the canonical curves in closer agreement with Walsh's assumptions. The dependence of the orbital energy on whether the orbital is occupied or vacant is less pronounced than for the canonical orbitals but still sufficient to cause the orbital energy plots to vary in appearance from molecule to molecule rather more than Walsh assumed.

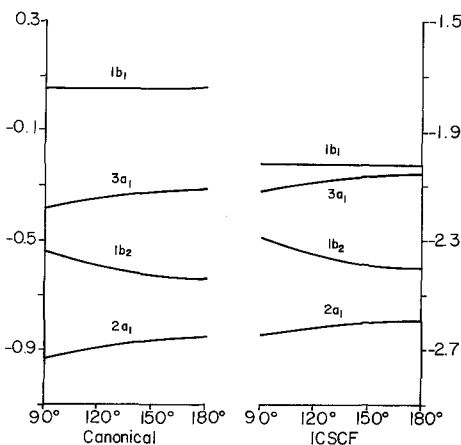
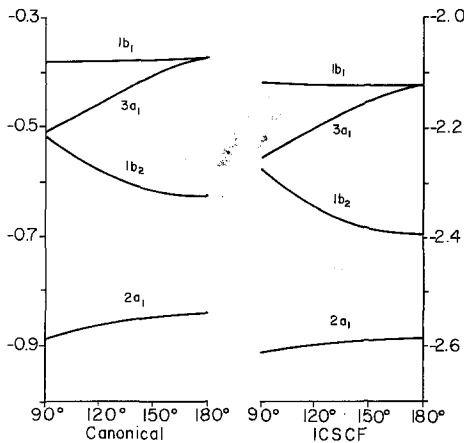
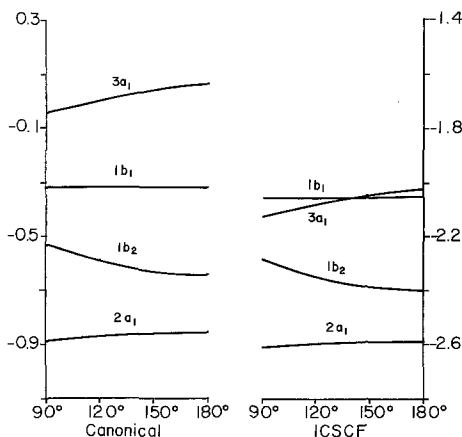
By definition, the sum of the ICSCF orbital energies is the SCF energy, so the only relevant question is whether the sum over only the valence orbitals correlates with the geometry. In the 25 examples considered here, the correlation was satisfactory for all 8 of the linear cases and 8 of the non-linear cases. In the remaining 9 non-linear cases, the bond angle was significantly overestimated. In these latter cases, however, this occurred because the energy curve was quite flat so that a small error in the energy caused a large deviation in the bond angle. On the whole, the ICSCF results are right about twice as often as the canonical results. There is no apparent qualitative difference between the cases where the ICSCF valence energy sum works and those where it does not. In almost every case the $1a_1$ orbital energy has a small positive slope so that omitting it leads systematically to too large a bond angle.

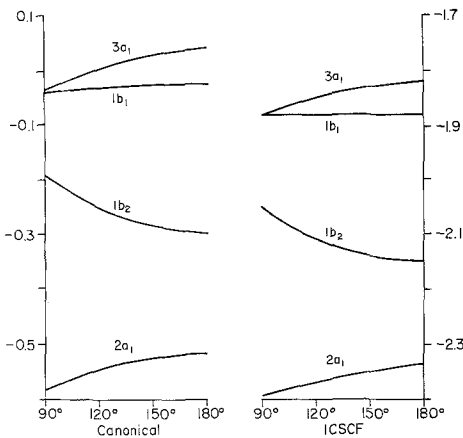
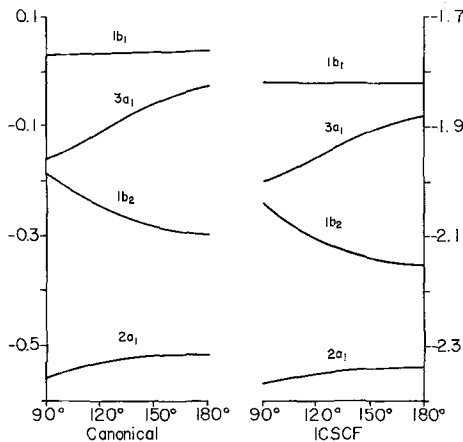
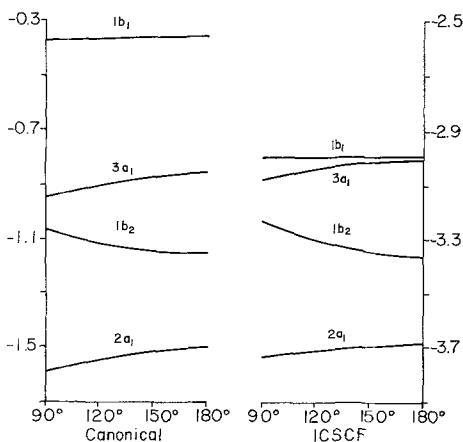
Because the results for AH₂ molecules tend to be too good [3], it is of interest to consider three other molecules: CO₂, Li₂O, and HCN. Carbon dioxide is a

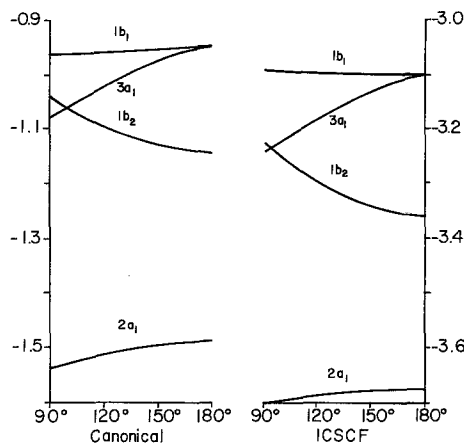
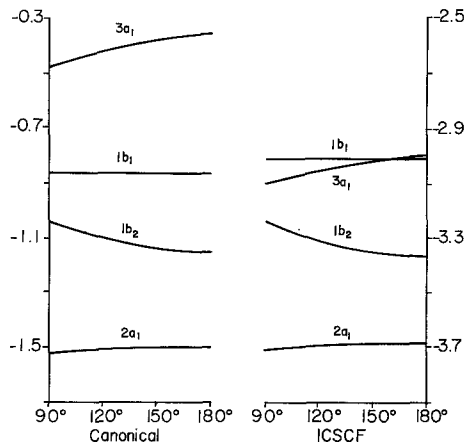
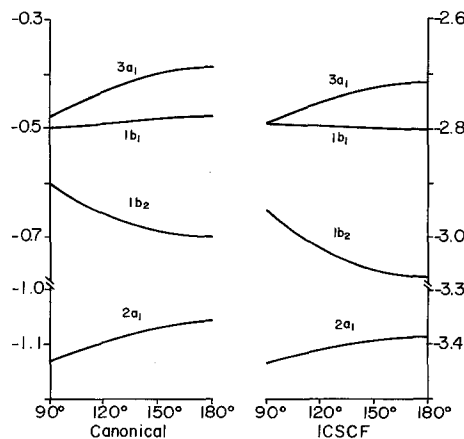
Fig. 1. Orbital energies for the $1a_1^2 2a_1^2 1b_2^2 1A_1$ state of BeH_2 Fig. 2. Orbital energies for the $1a_1^2 2a_1^2 1b_2^2 1A_1$ state of BH_2^+ Fig. 3. Orbital energies for the $1a_1^2 2a_1^2 1b_2^2 3a_1^2 2A_1$ state of BH_2

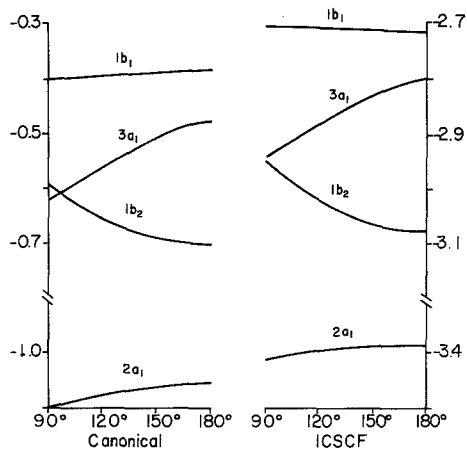
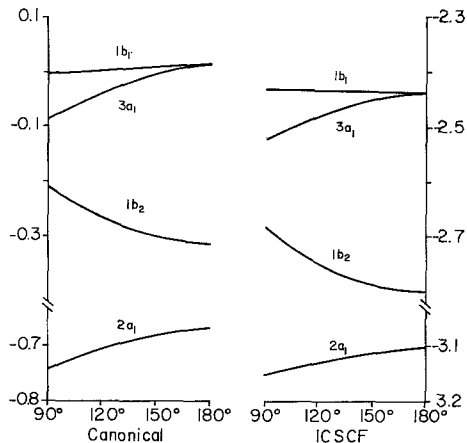
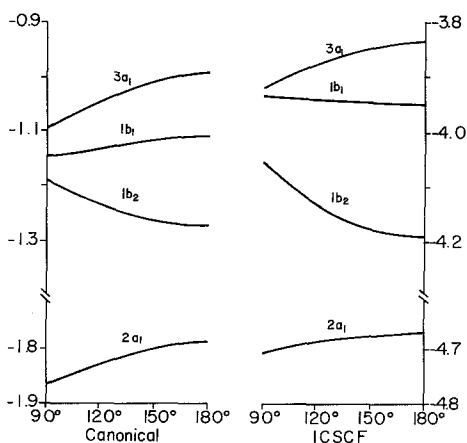
Fig. 4. Orbital energies for the $1a_1^2 2a_1^2 1b_2^2 1b_1^- 2B_1$ state of BH_2 Fig. 5. Orbital energies for the $1a_1^2 2a_1^2 1b_2^2 3a_1^2 1A_1$ state of BH_2^- Fig. 6. Orbital energies for the $1a_1^2 2a_1^2 1b_2^2 3a_1 1b_1^- 3B_1$ state of BH_2^-

Fig. 7. Orbital energies for the $1a_1^2 2a_1^2 1b_2^2 1b_1^2 1A_1$ state of BH_2^- Fig. 8. Orbital energies for the $1a_1^2 2a_1^2 1b_2^2 3a_1^2 2A_1$ state of CH_2^+ Fig. 9. Orbital energies for the $1a_1^2 2a_1^2 1b_2^2 1b_1^2 2B_1$ state of CH_2^+

Fig. 10. Orbital energies for the $1a_1^2 2a_1^2 1b_2^2 3a_1^2 1A_1$ state of CH_2 Fig. 11. Orbital energies for the $1a_1^2 2a_1^2 1b_2^2 3a_1 1b_1 3B_1$ state of CH_2 Fig. 12. Orbital energies for the $1a_1^2 2a_1^2 1b_2^2 1b_1^2 1A_1$ state of CH_2

Fig. 13. Orbital energies for the $1a_1^2 2a_1^2 1b_2^2 3a_1^2 1b_1^2 {}^2B_1$ state of CH_2^- Fig. 14. Orbital energies for the $1a_1^2 2a_1^2 1b_2^2 3a_1^2 1b_1^2 {}^2A_1$ state of CH_2^- Fig. 15. Orbital energies for the $1a_1^2 2a_1^2 1b_2^2 3a_1^2 {}^1A_1$ state of NH_2^+

Fig. 16. Orbital energies for the $1a_1^2 2a_1^2 1b_2^2 3a_1 1b_1$ 3B_1 state of NH_2^+ Fig. 17. Orbital energies for the $1a_1^2 2a_1^2 1b_2^2 1b_1^2$ 1A_1 state of NH_2^+ Fig. 18. Orbital energies for the $1a_1^2 2a_1^2 1b_2^2 3a_1^2 1b_1$ 2B_1 state of NH_2

Fig. 19. Orbital energies for the $1a_1^2 2a_1^2 1b_2^2 3a_1 1b_1^2 {}^2A_1$ state of NH_2 Fig. 20. Orbital energies for the $1a_1^2 2a_1^2 1b_2^2 3a_1^2 1b_1^2 {}^1A_1$ state of NH_2^- Fig. 21. Orbital energies for the $1a_1^2 2a_1^2 1b_2^2 3a_1^2 1b_1^2 {}^2B_1$ state of OH_2^+

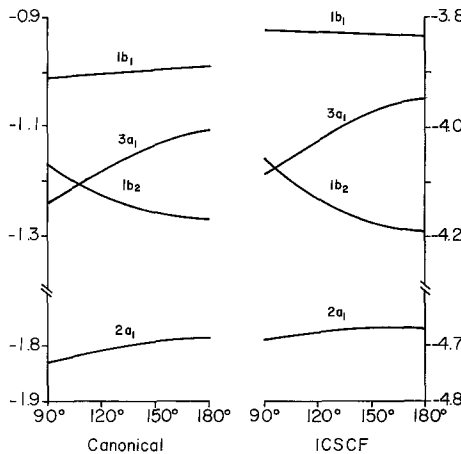


Fig. 22. Orbital energies for the $1a_1^2 2a_1^2 1b_2^2 3a_1 1b_1^2 2A_1$ state of OH_2^+

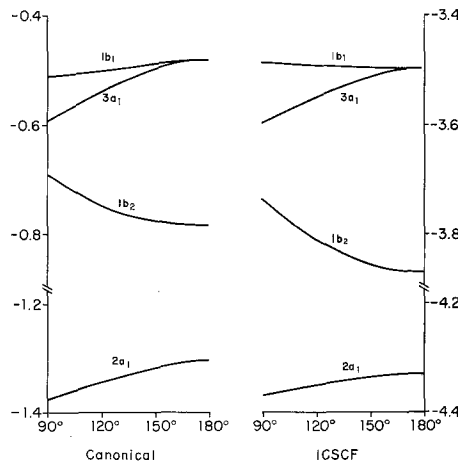


Fig. 23. Orbital energies for the $1a_1^2 2a_1^2 1b_2^2 3a_1^2 1b_1^2 1A_1$ state of OH_2

good example of an AB_2 system for which all theories work. Walsh's diagram, the canonical energies (Fig. 24a), and the ICSCF energies (Fig. 24b) are quite similar, and all predict a linear molecule. When considered in detail, it is seen that the $3a_1$ and $2b_2$ orbitals change with energy more than Walsh imagined, but their sum is nearly constant. The $4a_1$ orbital (analogous to the $2a_1$ orbital for AH_2) has a slight positive slope rather than the large negative slope predicted by Walsh. The $1b_1$ and $5a_1$ orbital energies are nearly constant in agreement with Walsh, but the slope of the $5a_1$ orbital has the opposite sign from his prediction. The $3b_2$ orbital is in the right place, and the slope has the predicted sign but a rather smaller magnitude. The $1a_2$, $4b_2$, and the ICSCF $6a_1$ and $2b_1$ are just as Walsh

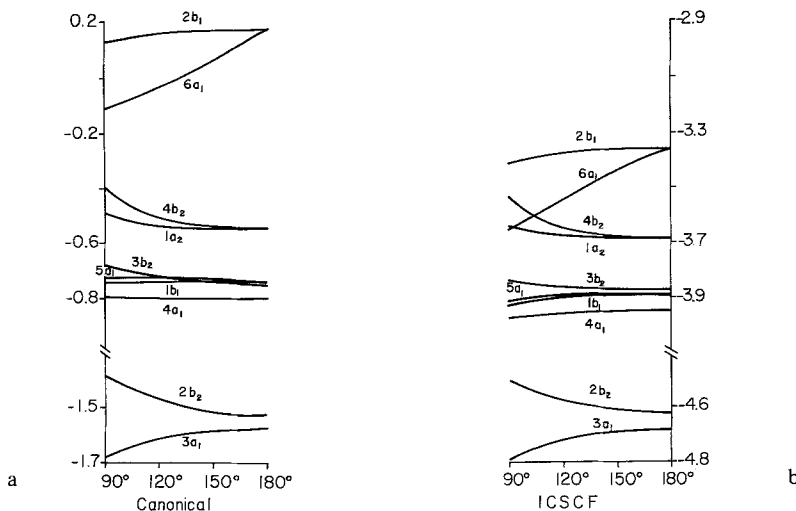


Fig. 24. a Canonical energies for the $1a_1^2 2a_1^2 1b_2^2 3a_1^2 2b_2^2 4a_1^2 1b_1^2 5a_1^2 3b_2^2 1a_2^2 4b_2^2 1A_1$ state of CO_2 . b ICSCF energies for the $1a_1^2 2a_1^2 1b_2^2 3a_1^2 2b_2^2 4a_1^2 1b_1^2 5a_1^2 3b_2^2 1a_2^2 4b_2^2 1A_1$ state of CO_2

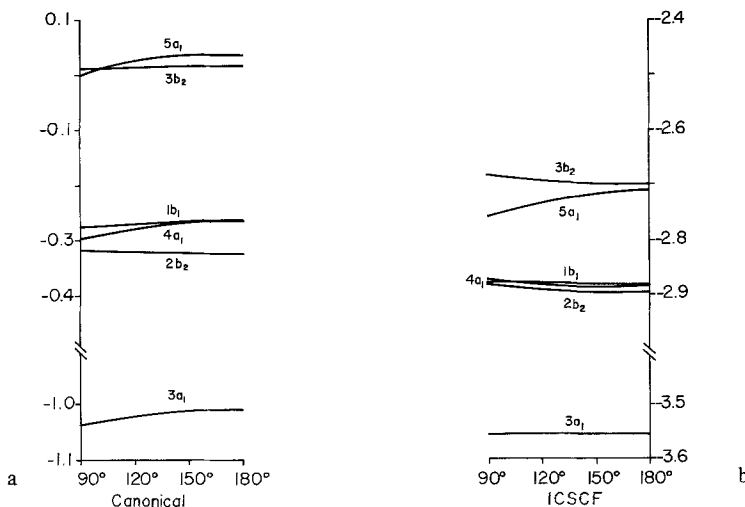


Fig. 25. a Canonical energies for the $1a_1^2 2a_1^2 1b_2^2 3a_1^2 2b_2^2 4a_1^2 1b_1^2 1A_1$ state of Li_2O . b ICSCF energies for the $1a_1^2 2a_1^2 1b_2^2 3a_1^2 2b_2^2 4a_1^2 1b_1^2 1A_1$ state of Li_2O

predicted. The molecule in this model is linear largely because of the $4b_2$ non-bonding π electrons.

The Li_2O molecule is formally similar to H_2O in its valence electron structure and hence should be bent in the Walsh model. The canonical orbital energy plot (Fig. 25a) resembles that for H_2O although the slope of the curves is much

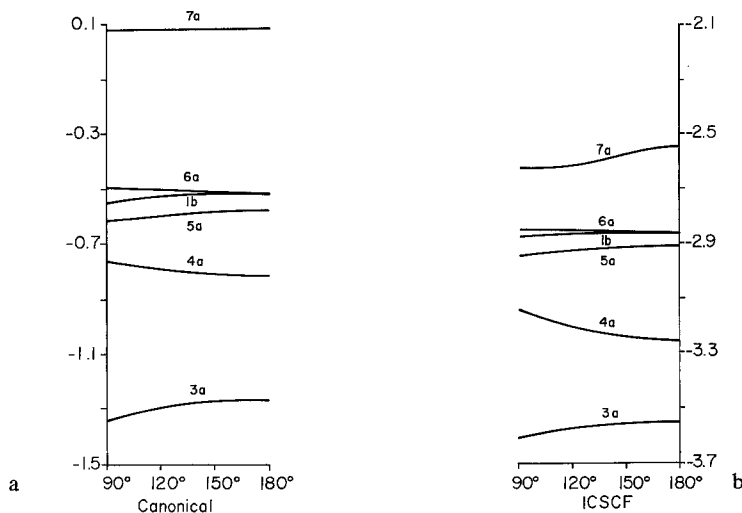


Fig. 26. a Canonical energies for the $1a^2 2a^2 3a^2 4a^2 5a^2 1b^2 6a^2 1A_1$ state of HCN. b ICSCF energies for the $1a^2 2a^2 3a^2 4a^2 5a^2 1b^2 6a^2 1A_1$ state of HCN

Table 26. The ground state of CO₂

	90	120	150	180	α_e
ICSCF					
$1a_1$	-23.4706	-23.5096	-23.5211	-23.5225	
$2a_1$	-14.5107	-14.4714	-14.4601	-14.4582	
$3a_1$	-4.7893	-4.7194	-4.6903	-4.6826	
$4a_1$	-3.9730	-3.9572	-3.9499	-3.9472	
$5a_1$	-3.9166	-3.8954	-3.8891	-3.8896	
$1b_2$	-23.4708	-23.5097	-23.5212	-23.5225	
$2b_2$	-4.4999	-4.5743	-4.6116	-4.6238	
$3b_2$	-3.8376	-3.8623	-3.8718	-3.8738	
$4b_2$	-3.5327	-3.6464	-3.6793	-3.6836	
$1b_1$	-3.9183	-3.8968	-3.8901	-3.8896	
$1a_2$	-3.6401	-3.6737	-3.6826	-3.6836	
$\Sigma_{\text{val}} \epsilon$	-64.3150	-64.4510	-64.5294	-64.5476	180
E	-187.1190	-187.4328	-187.5342	-187.5541	180
Canonical					
$1a_1$	-20.6163	-20.6601	-20.6763	-20.6767	
$2a_1$	-11.5110	-11.5027	-11.5076	-11.5079	
$3a_1$	-1.6834	-1.6130	-1.5839	-1.5733	
$4a_1$	-0.7964	-0.8017	-0.8021	-0.7982	
$5a_1$	-0.7278	-0.7237	-0.7349	-0.7390	
$1b_2$	-20.6164	-20.6602	-20.6764	-20.6767	
$2b_2$	-1.3730	-1.4659	-1.5134	-1.5262	
$3b_2$	-0.6793	-0.7203	-0.7387	-0.7404	
$4b_2$	-0.3932	-0.5063	-0.5410	-0.5456	
$1b_1$	-0.7440	-0.7376	-0.7398	-0.7390	
$1a_2$	-0.4923	-0.5325	-0.5459	-0.5456	
$\Sigma_{\text{val}} \epsilon$	-13.7788	-14.2020	-14.3994	-14.4146	180
$\Sigma_{\text{ali}} \epsilon$	-119.2662	-119.8480	-120.1200	-120.1372	180

Table 27. The ground state of Li₂O

	90	120	150	180	α_e
ICSCF					
1a ₁	-22.3983	-22.4000	-22.3981	-22.3975	
2a ₁	-5.1373	-5.1332	-5.1333	-5.1340	
3a ₁	-3.5546	-3.5569	-3.5567	-3.5562	
4a ₁	-2.8754	-2.8819	-2.8831	-2.8829	
1b ₂	-5.1355	-5.1328	-5.1332	-5.1340	
2b ₂	-2.8798	-2.8892	-2.8939	-2.8953	
1b ₁	-2.8782	-2.8813	-2.8828	-2.8829	
$\Sigma_{\text{val}} \epsilon$	-24.3760	-24.4186	-24.4330	-24.4346	180
E	-89.7184	-89.7507	-89.7624	-89.7654	180
Canonical					
1a ₁	-20.3532	-20.3408	-20.3312	-20.3281	
2a ₁	-2.4081	-2.3806	-2.3686	-2.3652	
3a ₁	-1.0338	-1.0200	-1.0106	-1.0070	
4a ₁	-0.2966	-0.2776	-0.2661	-0.2618	
1b ₂	-2.4062	-2.3801	-2.3686	-2.3651	
2b ₂	-0.3163	-0.3191	-0.3219	-0.3227	
1b ₁	-0.2751	-0.2695	-0.2641	-0.2618	
$\Sigma_{\text{val}} \epsilon$	-3.8436	-3.7724	-3.7254	-3.7066	< 90
$\Sigma_{\text{all}} \epsilon$	-54.1786	-53.9754	-53.8622	-53.8234	< 90

less steep. As discussed previously, for a molecule like H₂O or Li₂O where the H or Li carries a net positive charge, the sum of the canonical valence orbital energies gives too small a bond angle. In the case of Li₂O which is linear, this sum behaves just as it did for H₂O and shows no minimum above 90°. In the ICSCF model, the slope of each of the orbital energy curves (Fig. 25b) is slightly negative so the sum of the valence energies correctly predicts a linear molecule.

In the Walsh model, a molecule such as HCN is intermediate between AH₂ and AB₂. The 1a and 2a orbitals are 1s cores. The 3a orbital is supposedly analogous to 3a₁ and 2b₂, in the AB₂ system and was predicted by Walsh to not vary with angle. The 4a and 5a orbitals are the sigma bonds (analogous to 2a₁, 1b₂ in AH₂ or 4a₁, 3b₂ in AB₂). Walsh predicted both would have negative slopes in analogy to his predictions for AH₂ and AB₂ systems. Finally, the 1b and 6a orbitals are the π orbitals (analogous to 1b₁, 3a₁ in AH₂ or 1b₁, 5a₁ in AB₂). The 1b remains a π orbital in the bent molecule and was predicted to be independent of angle, while the 6a orbital energy was predicted to have a small negative slope. Based on this model, Walsh correctly predicted that HCN should be linear. The sum of the canonical valence orbital energies, on the other hand, incorrectly predicts that HCN is bent (the sum is still decreasing down to 90°). This is largely due to the positive slopes of the 3a and 5a orbitals (Fig. 26a). The ICSCF orbital energy picture (Fig. 26b) is qualitatively similar to the canonical energies with only slight changes in the magnitude of the slopes (particularly of the 4a orbital).

Table 28. The ground state of HCN

	90	120	150	180	α_e
ICSCF					
1a	-17.5783	-17.5734	-17.5672	-17.5651	
2a	-13.3603	-13.3761	-13.3854	-13.3881	
3a	-3.6057	-3.5707	-3.5559	-3.5520	
4a	-3.1404	-3.2057	-3.2433	-3.2555	
5a	-2.9428	-2.9248	-2.9148	-2.9114	
6a	-2.8485	-2.8574	-2.8649	-2.8642	
1b	-2.8724	-2.8675	-2.8627	-2.8643	
$\Sigma_{\text{val}} \varepsilon$	-30.8196	-30.8522	-30.8832	-30.8948	180
E	-92.6970	-92.7512	-92.7884	-92.8009	180
Canonical					
1a	-15.6741	-15.6533	-15.6420	-15.6388	
2a	-11.3286	-11.3316	-11.3367	-11.3387	
3a	-1.3381	-1.2895	-1.2714	-1.2673	
4a	-0.7627	-0.7901	-0.8083	-0.8144	
5a	-0.6162	-0.5906	-0.5808	-0.5782	
6a	-0.4941	-0.5030	-0.5106	-0.5130	
1b	-0.5480	-0.5248	-0.5154	-0.5131	
$\Sigma_{\text{val}} \varepsilon$	-7.5022	-7.3960	-7.3730	-7.3720	< 90
$\Sigma_{\text{all}} \varepsilon$	-61.5076	-61.3658	-61.3304	-61.3270	< 90

Table 29. The $1a_1^2 2a_1^2 1e^4 1A_1$ state of BH_3

	90	100	110	120	α_e
ICSCF					
1a ₁	-8.2158	-8.2094	-8.2022	-8.1949	
2a ₁	-1.8189	-1.8080	-1.8004	-1.7953	
1e	-1.5404	-1.5622	-1.5806	-1.5962	
3a ₁	-1.3629	-1.3459	-1.3241	-1.2983	
$\Sigma_{\text{val}} \varepsilon$	-9.7994	-9.8648	-9.9232	-9.9754	120
E	-26.2309	-26.2835	-26.3278	-26.3651	120
Canonical					
1a ₁	-7.6331	-7.6284	-7.6245	-7.6209	
2a ₁	-0.7417	-0.7252	-0.7139	-0.7063	
1e	-0.4399	-0.4605	-0.4795	-0.4963	
3a ₁	-0.0023	0.0155	0.0359	0.0591	
$\Sigma_{\text{val}} \varepsilon$	-3.2430	-3.2924	-3.3458	-3.3978	120
$\Sigma_{\text{all}} \varepsilon$	-18.5092	-18.5492	-18.5948	-18.6396	120

Yet these small quantitative changes are sufficient so that the ICSCF valence orbital energies correctly predict the molecule to be linear.

Calculations have also been carried out on some AH_3 molecules with less satisfactory results. For these molecules it takes a rather sophisticated basis

Table 30. The $1a_1^2 2a_1^2 1e^4 1A_1$ state of CH_3^+

	90	100	110	120	α_e
ICSCF					
$1a_1$	-12.3907	-12.3891	-12.3863	-12.3829	
$2a_1$	-2.6436	-2.6308	-2.6210	-2.6135	
$1e$	-2.2384	-2.2630	-2.2838	-2.3015	
$3a_1$	-2.0767	-2.0590	-2.0375	-2.0131	
$\Sigma_{\text{val}} \varepsilon$	-14.2408	-14.3136	-14.3772	-14.4330	120
E	-39.0221	-39.0916	-39.1499	-39.1989	120
Canonical					
$1a_1$	-11.6892	-11.6867	-11.6849	-11.6833	
$2a_1$	-1.3125	-1.2943	-1.2806	-1.2702	
$1e$	-0.8885	-0.9093	-0.9287	-0.9462	
$3a_1$	-0.3643	-0.3405	-0.3143	-0.2853	
$\Sigma_{\text{val}} \varepsilon$	-6.1790	-6.2258	-6.2760	-6.3250	120
$\Sigma_{\text{all}} \varepsilon$	-29.5664	-29.5992	-29.6458	-29.6916	120

Table 31. The $1a_1^2 2a_1^2 1e^4 3a_1^2 2A_1$ state of CH_3

	90	100	110	120	α_e
ICSCF					
$1a_1$	-12.1692	-12.1685	-12.1671	-12.1655	
$2a_1$	-2.4545	-2.4391	-2.4271	-2.4179	
$1e$	-2.0467	-2.0718	-2.0937	-2.1134	
$3a_1$	-2.0015	-1.9764	-1.9442	-1.9022	
$\Sigma_{\text{val}} \varepsilon$	-15.0973	-15.1418	-15.1732	-15.1916	120
E	-39.4355	-39.4787	-39.5074	-39.5227	120
Canonical					
$1a_1$	-11.2286	-11.2233	-11.2186	-11.2146	
$2a_1$	-0.9488	-0.9250	-0.9062	-0.8912	
$1e$	-0.5081	-0.5268	-0.5443	-0.5605	
$3a_1$	-0.4766	-0.4477	-0.4134	-0.3699	
$\Sigma_{\text{val}} \varepsilon$	-4.4066	-4.4049	-4.4030	-4.3943	< 90
$\Sigma_{\text{all}} \varepsilon$	-26.8638	-26.8515	-26.8402	-26.8235	< 90

set to get the geometry reliably (rather than accidentally) correct at the SCF level. For BH_3 , CH_3^+ , CH_3 , OH_3^+ and NH_3^+ the basis set of the quality used here gives the presumably correct planar geometry as judged by other calculations and experimental evidence. But this basis set also gives planar geometry for NH_3 . With this difficulty in mind, the RHF and ICSCF results can be compared. For

Table 32. The $1a_1^2 2a_1^2 e^4 3a_1$ state of NH_3^+

	90	100	110	120	α_e
ICSCF					
$1a_1$	-17.1841	-17.1846	-17.1832	-17.1801	
$2a_1$	-3.4483	-3.4339	-3.4228	-3.4147	
$1e$	-2.8954	-2.9232	-2.9480	-2.9706	
$3a_1$	-2.8857	-2.8574	-2.8225	-2.7790	
$\Sigma_{\text{val}} \epsilon$	-21.3642	-21.4180	-21.4601	-21.4908	120
E	-55.7320	-55.7871	-55.8262	-55.8511	120
Canonical					
$1a_1$	-16.0118	-16.0048	-15.9971	-15.9875	
$2a_1$	-1.5793	-1.5559	-1.5361	-1.5189	
$1e$	-1.0044	-1.0218	-1.0375	-1.0511	
$3a_1$	-1.0248	-0.9935	-0.9581	-0.9158	
$\Sigma_{\text{val}} \epsilon$	-8.2010	-8.1925	-8.1803	-8.1581	< 90
$\Sigma_{\text{all}} \epsilon$	-40.2246	-40.2021	-40.1745	-40.1331	< 90

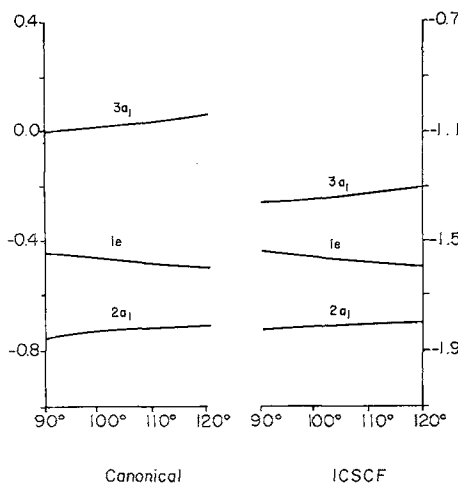
Table 33. The $1a_1^2 2a_1^2 e^4 3a_1^2$ state of NH_3

	90	100	110	120	α_e
ICSCF					
$1a_1$	-16.9616	-16.9608	-16.9582	-16.9542	
$2a_1$	-3.2370	-3.2174	-3.1991	-3.1804	
$1e$	-2.6772	-2.7036	-2.7265	-2.7462	
$3a_1$	-2.4978	-2.4819	-2.4661	-2.4526	
$\Sigma_{\text{val}} \epsilon$	-22.1784	-22.2110	-22.2364	-22.2508	120
E	-56.1014	-56.1346	-56.1527	-56.1589	120
Canonical					
$1a_1$	-15.5449	-15.5356	-15.5247	-15.5122	
$2a_1$	-1.1917	-1.1624	-1.1340	-1.1047	
$1e$	-0.5929	-0.6084	-0.6212	-0.6308	
$3a_1$	-0.4444	-0.4213	-0.3991	-0.3794	
$\Sigma_{\text{val}} \epsilon$	-5.6438	-5.6010	-5.5510	-5.4914	< 90
$\Sigma_{\text{all}} \epsilon$	-36.7336	-36.6722	-36.6004	-36.5158	< 90

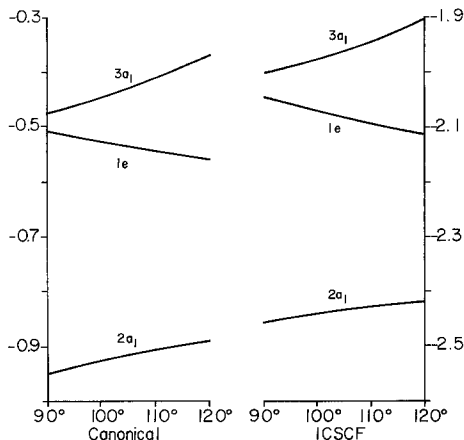
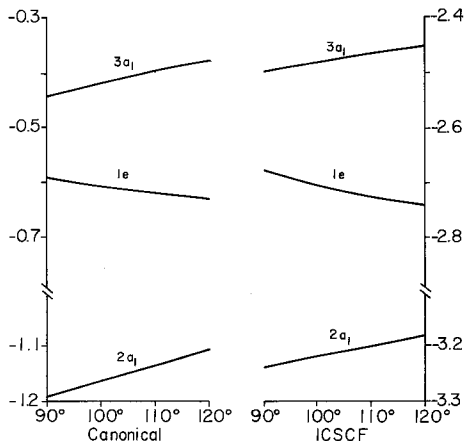
all these molecules the ICSCF valence orbital energy sum predicted a planar geometry in agreement with E_{SCF} . But the slope of e_{1s} is large enough to make this sum continue to predict a planar geometry even for better basis sets for NH_3 . The sum of the RHF valence energies is still worse, however, since it would predict that CH_3 , NH_3^+ , NH_3 , and OH_3^+ were all bent to a HAH angle of less

Table 34. The $1a_1^2 2a_1^2 e^4 3a_1^2 {}^1A_1$ state of H_3O^+

	90	100	110	120	α_e
ICSCF					
$1a_1$	-22.7984	-22.7965	-22.7922	-22.7860	
$2a_1$	-4.4104	-4.3933	-4.3773	-4.3615	
$1e$	-3.6841	-3.7126	-3.7375	-3.7593	
$3a_1$	-3.5233	-3.5057	-3.4887	-3.4735	
$\Sigma_{\text{val}} e$	-30.6038	-30.6484	-30.6820	-30.7072	120
E	-76.2004	-76.2411	-76.2663	-76.2793	120
Canonical					
$1a_1$	-21.0404	-21.0254	-21.0084	-20.9894	
$2a_1$	-1.8963	-1.8657	-1.8356	-1.8049	
$1e$	-1.1422	-1.1537	-1.1628	-1.1692	
$3a_1$	-1.0246	-0.9986	-0.9738	-0.9511	
$\Sigma_{\text{val}} e$	-10.4106	-10.3434	-10.2700	-10.1888	< 90
$\Sigma_{\text{all}} e$	-52.4915	-52.3942	-52.2868	-52.1676	< 90

Fig. 27. Orbital energies for the $1a_1^2 2a_1^2 1e^4 3a_1^2 {}^1A_1$ state of BH_3

than 90° . The orbital energy versus bond angle diagrams (Fig. 27-29) for all these molecules for both the canonical and ICSCF results are similar to those predicted by Walsh and previously reported [7].

Fig. 28. Orbital energies for the $1a_1^2 2a_1^2 1e^4 3a_1$ 2A_1 state of CH_3 Fig. 29. Orbital energies for the $1a_1^2 2a_1^2 1e^4 3a_1$ 1A_1 state of NH_3

Acknowledgement. The authors wish to acknowledge the financial support of the National Science Foundation.

References

1. Mulliken, R. S.: Rev. Mod. Phys. **14**, 204 (1942)
2. Walsh, A. D.: J. Chem. Soc. (London) 2260, **1953**
3. Peyerimhoff, S. D., Buenker, R. J.: To be published. The authors wish to thank Dr. Peyerimhoff for providing us with an advance copy of this manuscript
4. Allen, L. C.: Theoret. Chim. Acta (Berl.) **24**, 117 (1972)
5. Coulson, C. A., Neilson, A. H.: Discussions Faraday Soc. **35**, 71 (1963)
6. Buenker, R. J., Peyerimhoff, S. D.: J. Chem. Phys. **45**, 3682 (1966)
7. Peyerimhoff, S. D., Buenker, R. J., Allen, L. C.: J. Chem. Phys. **45**, 734 (1966)
8. Moskowitz, J. W., Harrison, M. C.: J. Chem. Phys. **43**, 3550 (1965)
9. Davidson, E. R.: J. Chem. Phys. **57**, 1999 (1972)
10. Whitten, J. L.: J. Chem. Phys. **44**, 359 (1966)
11. Krauss, M.: J. Res. Nat. Bur. Std. **68** A, 635 (1964)

Prof. Dr. E. R. Davidson, —chemistry Department BG-10
University of Washington, Seattle, Washington 98195, USA